Hindawi
International Journal of Aerospace Engineering
Volume 2021, Article ID 3290518, 12 pages
https://doi.org/10.1155/2021/3290518

Research Article

Design Optimization and Burst Speed Prediction of a Ti2AlNb Blisk

Yue Guo, Yi-xiong Liu, Yun-wu Wu, Hang Cao, and Da Mo

AECC Shenyang Engine Research Institute, Shenyang 110015, China

Correspondence should be addressed to Yi-xiong Liu; yixiong.liu5021@gmail.com

Received 11 June 2021; Accepted 20 September 2021; Published 4 October 2021

Academic Editor: Marco Morandini

The increasing demand for power, fuel efficiency, and safety of aeroengines has called for weight reduction and structural integrity examination of the critical components. This paper is aimed at performing a systematic investigation on the design of a high-speed Ti2AlNb blisk, including disc geometry optimization and burst speed prediction. Incorporating the design of the experimental approach and the commercial software has guaranteed that the optimization could be accomplished. Six key parameters were defined as variables with regard to the geometric dimensions whereas the safety factors were set as constraints to make the disc feasible. Sensitivity analysis has been conducted to study the effects of the variables on the safety factors and disc weight. Bore width, web width, and bore angle are identified to be the dominant factors regarding optimization. Results reveal that the bore width and web width are positively related to the safety factors at the cost of increasing the disc weight. On the contrary, the effects of the bore angle show the opposite trend. Finally, the achieved minimum disc weight is 15.2 kg with all the safety factors meeting the requirements. Upon completing the disc shape optimization, the burst speed was estimated using three elaborated methods. The comparisons between the numerical results and the experimental results indicate that the mean stress method is accurate when the correction coefficient is chosen properly. The local stress and strain method and the global plastic instability method also offer a precise prediction on the burst speed with errors of less than 5%. It could also be concluded that the predicted web failure in the radial direction of the disc is in good agreement with the experimental results.

1. Introduction

The application of new materials and new structures in aeroengines has made it more difficult to assess engine safety. The desire to design a higher performance engine within a limited design iteration drives the engineers to further implement advanced approaches and integrated tools to estimate the reliability and integrity of the key components. The blisk structure has cancelled the conventional tenon connection and incorporates the blades as an integrated structure, which could reduce the rotor weight and blade counts as well as eliminate the flow loss [1]. The posing issue is that the high cycle life and vibration problems are outstanding due to the absence of an effective damper. However, the approaches of the conventional disc in terms of optimization strategy are still applicable.

Numerous researchers have performed engine component design optimization to achieve the optimal structure. Kasina et al. [2] conducted an optimization design aiming at the minimum weight of a fir tree connection turbine disc with several critical parameters regarding the disc dimensions which were identified as variables. Xiaodong and Xiuli [3] developed a turbine disc design process based on Ansys Workbench software and considered the aerodynamic, thermal, and structural coupling effects. Rao et al. [4], Li and Lu [5], and Lu and Lu [6] have undertaken a similar engine disc optimization investigation with remarkable results. In recent years, more designers are dedicated to utilizing the design of experiment (DOE) approach to search for the optimal strategy. Liu et al. [7] analyzed the fan shroud failure causes and performed shroud optimization to mitigate the contact stress concentration with the DOE method. The maximum contact stress dropped dramatically from 623 MPa to 378 MPa. Huang et al. [8] adopted the kriging surrogate models into the turbine disc optimization process. The corresponding results showed that the kriging appropriation offered high

accuracy but low computation time. Bharatish et al. [9] implemented Taguchi's DOE approach into the optimization of a turbine disc fir tree joint for fretting analysis purposes. Mavroudi et al. [10] investigated the shape optimization of the blade and disc fixing by simultaneously updating the model and calculating the stress. The DOE approach has provided the designers with a fast and accurate way to obtain the desired structure, which shortens the design iterations and improve efficiency.

After obtaining the optimal blisk shape, another concern that has drawn attention is the burst speed prediction. Aeroengines have to cater to extreme conditions resulting in a complex and challenging working environment for the key components, especially the military fighters which call for high power demand and operating flexibility. The consequence is that the compressor blisk sometimes rotates at very high speed, bearing the centrifugal load, and the rear stages even endure the high temperature, uneven temperature, and corrosion. The integrity of the compressor blisk is crucial for engine safety. Once broken, the fragments would break through the casing and even penetrate the fuel tank and the cockpit, leading to severe and catastrophic consequences [11]. Many studies have been carried out to predict the burst speed by miscellaneous approaches. Manavi [12] investigated the burst of a centrifugal rotor by 2D and 3D finite element analysis with a mean stress comparison approach and test validation. The rupture results revealed that the crack initiated from the slots which are always the weak points of the blisk. Maziere [13] compared the quasistatic and dynamic prediction on overburst speed and found that the Hosford yield criterion was accurate with only 0.1% error compared to the experimental results. More importantly, the local plastic strain is strongly dependent on the yield function. Servetnik [14] performed a numerical calculation on the HPT disc with the finite element analysis based on the energy method. It was proved that the Tresca yield criterion was better than the von Mises yield criterion in predicting the limit speed. Ekhteraei Toussi and Rezaei [15] implemented the elastic-plastic imaging method to obtain the limit speed by observing the deformation of the disc. What is interesting is that the inside part seemed to encounter failure first in the radial direction due to the higher equivalent stress.

There are many factors affecting the accuracy of burst speed prediction, consisting of the geometric parameters, load conditions, and material properties. Kasina et al. [2] investigated the influences of the critical dimensions on the burst speed margin, such as the bore radius and bore width. The increase of bore radius would significantly increase the burst margin whereas the expansion of bore width had an adverse effect on the burst limit. Maruthi et al. [16] analyzed the influences of different load conditions including the centrifugal load, thermal load, and blade load on burst margin. With the real loading conditions, the burst speed is much lower than the simple centrifugal load condition. Squarcella et al. [17] performed a sensitivity analysis of the material properties on the burst speed of turbine discs. The stress-strain curve plot was significantly affected by the Young modulus, ultimate stress values, ultimate strain values, stiffness, and yield stress, which would impact the burst speed estimation.

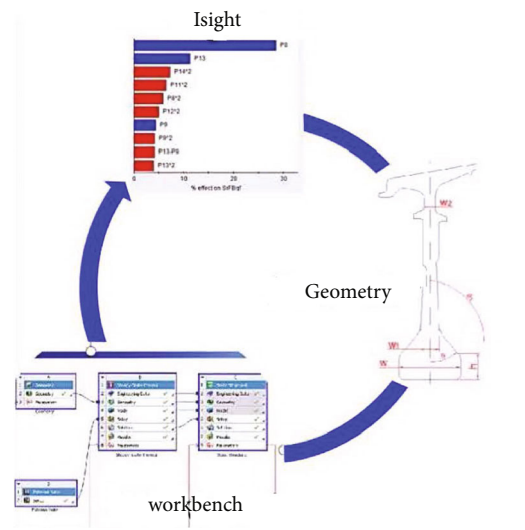

Figure 1: Design optimization framework.

This paper presents a consistent and coherent investigation on the design optimization, burst speed estimation, and validation of a Ti2AlNb blisk. The DOE method was adopted in the design process with the integration of Workbench and Isight software. Sensitivity analysis regarding the critical geometric parameters was established to search for the most influential factors that provide the minimum weight and stress. The burst speed was predicted by three approaches using the finite element results on obtaining the optimum disc shape. Finally, the blisk burst experiment was conducted to validate the numerical results.

2. Design Optimization

This chapter first describes the design process and the methodology implemented in the disc optimization. Then, the effects of the critical parameters on the disc weight and safety factor were demonstrated by the Pareto bar chart. Afterwards, the optimization results were checked against the initial values.

2.1. Methodology. A brief design framework is depicted in Figure 1. It consists of three individual procedures, which are mutually connected. The initial weight and stress could be calculated in the Workbench software. Meanwhile, the critical geometric parameters have been established as variables with the identified lower and upper bounds. By setting up appropriate design constraints and design objectives, the optimal disc shape could be achieved with minimum weight by the DOE approach. In Workbench, the geometry module, thermal analysis module, and static strength analysis module are employed to conduct the optimization. The disc geometry is updated according to the optimized sampling data from Isight. Therefore, the optimum disc shape and stress would be obtained concurrently without too many iterations.

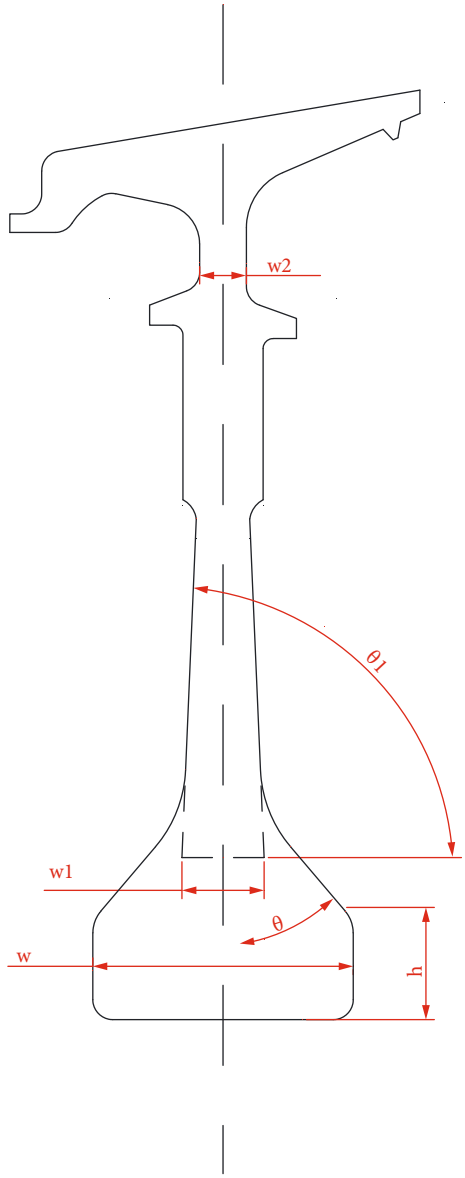

Figure 2: Design variables.

2.2. Design Space Exploration. In the majority of disc optimization cases, several objectives have to be achieved simultaneously. Therefore, it is required to identify the most influential parameters for the design objectives. In this scenario, six parameters were chosen as variables, as shown in Figure 2. The bore height, bore width, and bore angle are crucial for the bore stress distribution and deformation. Meanwhile, the neck width is responsible for the neck area which is thin and needs careful design. The blade is designed as an equivalent mass module. Table 1 lists the boundaries of the six variables according to the approximate layout of disc and the compatibility. Another important issue that has to be considered in the actual engineering design [18–20] is the space constraints especially the bore radius concern. In this scenario, the bore radius is kept constant to prevent possible interference and rub risk.

Table 1: Definition of design variables.

Variables	Meaning	Lower bound	Upper bound
h (P11)	Bore height	9 mm	12 mm
w_2 (P12)	Neck width	7 mm	12 mm
θ_1 (P13)	Web angle	78°	82°
θ (P14)	Bore angle	38°	42°
w_1 (P8)	Web width	6 mm	12 mm
w (P9)	Bore width	38 mm	44 mm

Table 2: Design constraints.

Constraints	Initial values	Desired values
BCS	1.01	1.05
CSCS	1.31	1.25
CRS	1.57	1.35
MPCS	1.39	1.35

The design optimization could be formulated as a weight minimization problem, as shown in (1). The main aim is to find the minimum weight within the design space but maintaining the safety factors above the required level. $\sigma_{0.2,\mathrm{b}}$ (T_θ) and $\sigma_{0.2,\mathrm{b}}$ (T_r) refer to the circumferential stress and radial stress receptively while the $n_{\theta,0.2,\mathrm{b}}$ and the $n_{r,0.2,\mathrm{b}}$ are the corresponding safety factors.

$$\left.\begin{aligned} &\text{Find}: \min{}_{\text{weight}}(h, \theta_i, w_i) \\ &\frac{\sigma_{0.2,b}(T_\theta)}{\overline{\sigma_\theta}} \geq n_{\theta,0.2,b}, \\ &\frac{\sigma_{0.2,b}(T_r)}{\overline{\sigma_r}} \geq n_{r,0.2,b}. \end{aligned}\right\} \tag{1}$$

Before moving to the design objectives, it is important to define the design constraints to make the optimized disc more practical and achievable. For the investigated compressor blisk, the design priority is to guarantee that the blisk would still maintain its integrity under the burst speed requirement. Correspondingly, the maximum stress and safety factors have to be lying within a certain range. The safety factors of bore circumferential stress (BCS), cylindrical surface circumferential stress (CSCS), cylindrical radial stress (CRS), and meridian plane circumferential stress (MPCS) are identified as design constraints, as listed in Table 2. It could be seen that the initial values of the safety factors are higher than the desired values except the BCS, indicating that there is still much space for improvement.

The main objective of this paper is to obtain the optimum disc with minimum weight. To carry out the optimization, Ansys Workbench and Isight were employed to achieve the desired objective.

2.3. Sensitivity Analysis. In order to explore the influences of the variables on the results, the optimal Latin hypercube design (OLHD) method was implemented to generate the design space. The OLHD method will create distributed

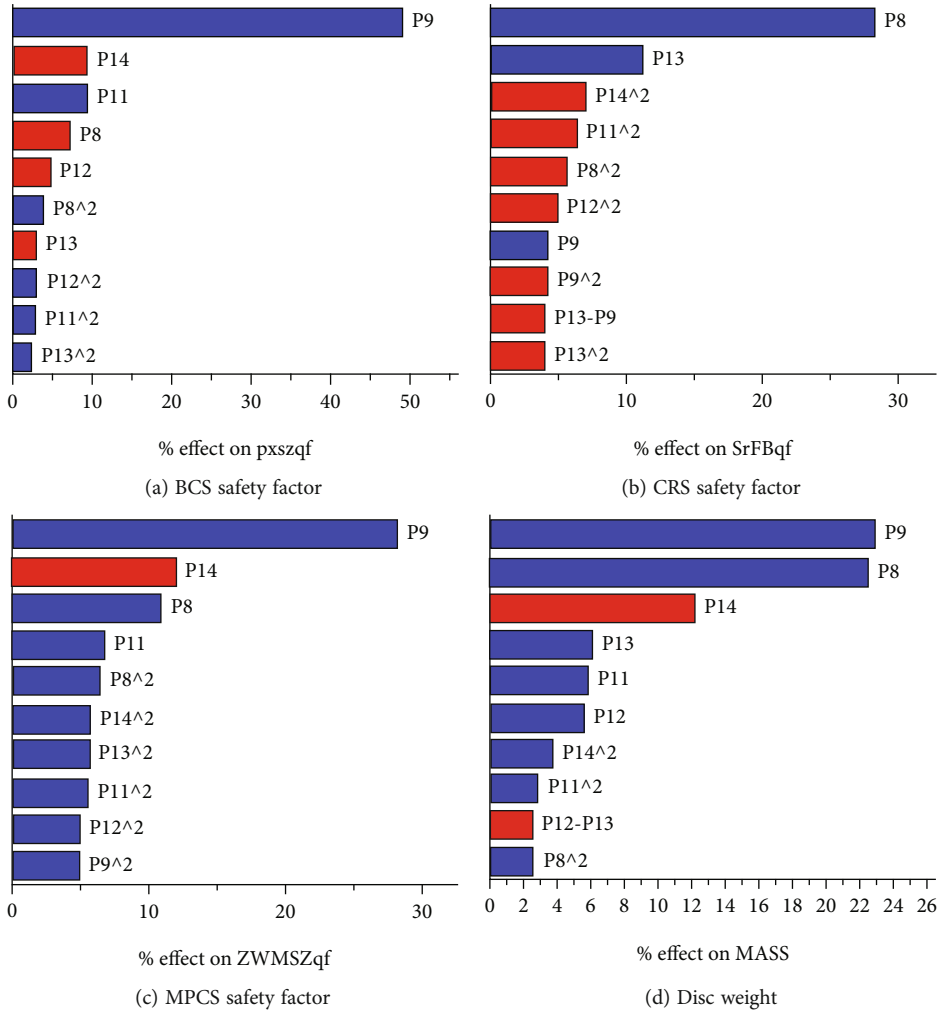

Figure 3: Pareto plots.

sampling points in the design space so as to guarantee that the points are uniformly located. Consequently, it ensures that the design variables and surface response are accurately simulated. The number of the sampling points was chosen as 25.

A multivariate quadratic regression model was adopted to assess the effects of each variable, as shown in (2). It should be noted that the input has been normalized to [-1, +1]. After obtaining the model coefficients, they were converted into percentages representing the contribution rate, as listed in (3).

$$y = \beta_0 + \sum \beta_i x_i + \sum \beta_i x_i^2 + \sum \beta_i x_i x_j, \tag{2}$$

$$N_{xi}(\%) = \frac{100 S_{xi}}{\sum S_{xi}}. \tag{3}$$

Figure 3 depicts the Pareto bar charts of the variables on the disc weight and safety factors. The red bar indicates that the parameters demonstrate a positive response, whereas the red bar reveals that the parameters would weaken the objectives. From Figure 3(a), it is evident that the bore width (P9) is the most influential factor contributing almost 50% to the BCS safety factor. It means that a larger P9 is desired due to the fact that BCS is lower than the target value, as discussed previously. Following is the bore height (P11) which takes up about 9% contribution on BCS. Nevertheless, a closer inspection of the figure shows that bore angle (P14) is negative on the BCS, meaning that it should be lowered to increase the safety factor.

A similar trend could be observed in Figures 3(c) and 3(d). The contribution of bore width ranks top on the MPCS safety factor and disc weight while the bore angle shows the largest negative response. What needs to be pointed out is that the decrease of web width (P8) could also dramatically reduce disc weight but at the risk of lowering the MPCS safety factor. For the CRS safety factor, it is clear that the web width and web angle are the two dominant factors that proportionally related.

From the above discussion, it could be concluded that the bore width and web width are the key parameters that could improve the safety factors but burden the disc weight. On the contrary, the increase of the bore angle would lessen the weight but impact the safety factors. The optimum disc shape needs trade off among the variables.

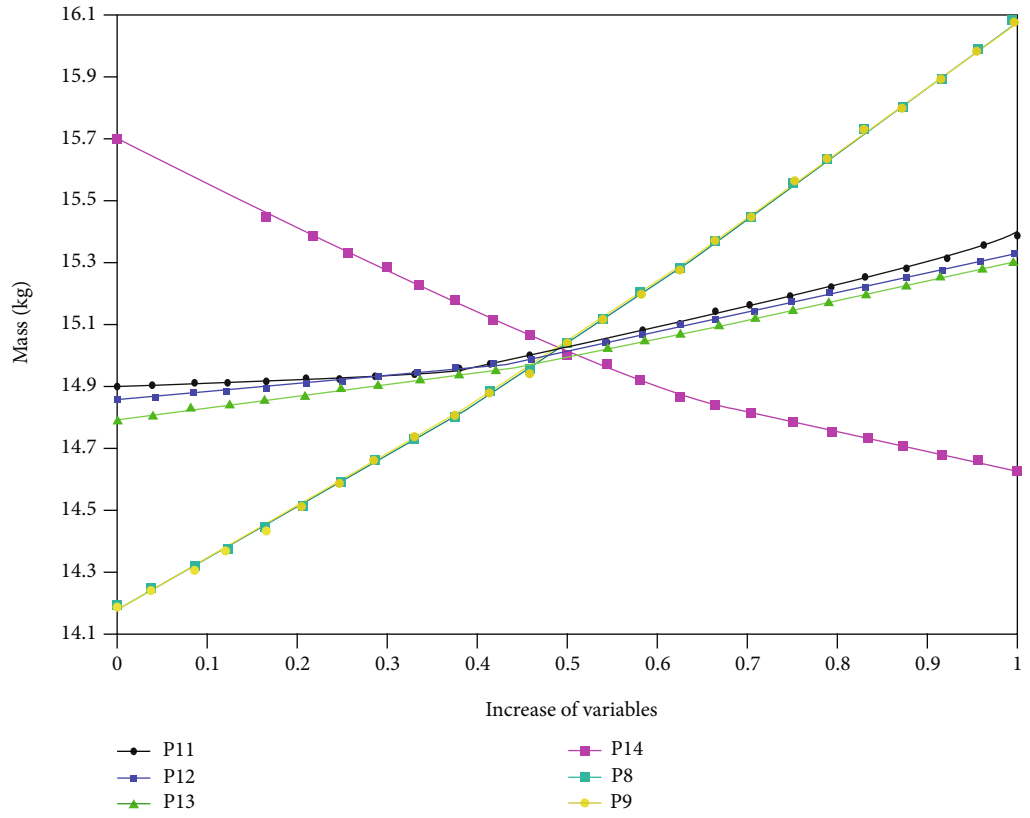

Figure 4: Effects of variables on the disc weight.

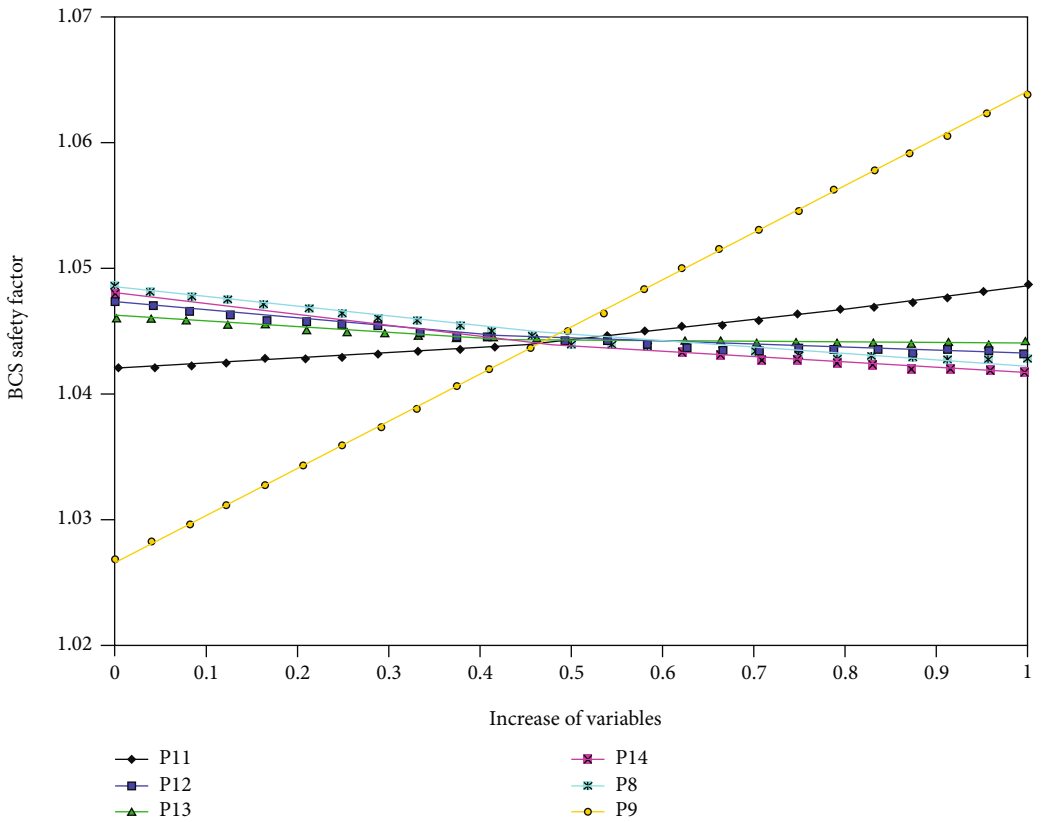

Figure 5: Effects of variables on the BCS safety factor.

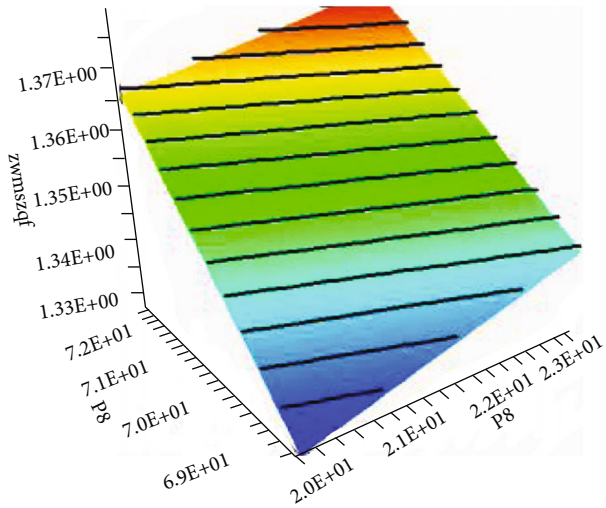

Figure 6: BCS safety factor response surface.

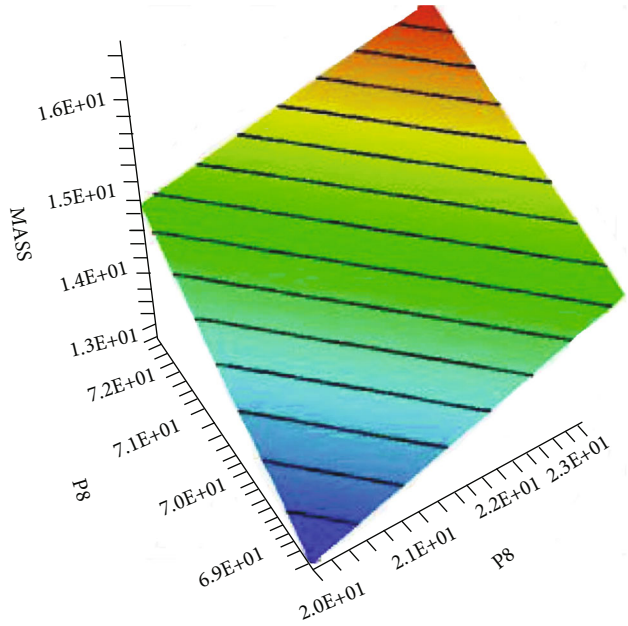

Figure 7: Disc weight response surface.

A more specific analysis was demonstrated in Figures 4 and 5, which illustrate the influences of each variable on the disc weight and BCS safety factor in quantity. The weight reduction reaches 6.37% when the bore angle is doubled. However, the corresponding BCS safety factor is lower than the desired value, indicating a compromise in the stress and weight. More importantly, when the bore width or the web width is twice larger, then the disc is 11.9% heavier than the initial value. Nevertheless, the web width increase results in the drop of BCS safety factor and should be avoided, as shown in Figure 5. The rise of bore width and bore height is beneficial for the BCS safety factor, which contribute 3.6% and 0.6%, respectively. Other parameters show less relevance in the weight and safety factor optimization.

Table 3: Optimum design variables.

Variables	Optimum values
h (P11)	10 mm
w_2 (P12)	10 mm
θ_1 (P13)	82°
θ (P14)	40°
w_1 (P8)	8 mm
w (P9)	39 mm

Table 4: Optimum solution.

Constraints	Initial values	Optimum values
BCS	1.01	1.05
CSCS	1.31	1.27
CRS	1.57	1.35
MPCS	1.39	1.35
Disc weight (kg)	16.5	15.2

2.4. Result Analysis. The response surface was plotted based on the sampling points generated by the OLHD approach, as depicted in Figures 6 and 7. Obviously, there exist optimum parameters that offer the lowest achievable weight and adequate safety factor. The optimal variables are listed in Table 3. The effects of the variables are mutually affected requiring compromise to minimize the weight with the constrained space and given constraints.

The best solution was then obtained by finite element analysis with the optimal variables, as listed in Table 4. It is clear that the BCS safety factor has reached the desired values while other safety factors have been reduced to cater for the BCS. In addition, the disc weight has dropped from 16.5 to 15.2 kg, reaching almost a 7.88% reduction. It would be helpful in minimizing the whole engine weight and hence decrease the mission fuel burn. The optimization approach utilized in this paper provides users with easier access and fewer iterations for compressor disc shape optimization. It could also include the thermal load, centrifugal load, and blade load affecting the disc stress in one platform.

3. Burst Speed Prediction

The application of Ti2AlNb material in areoengines has significantly improved the endurance temperature from the maximum of 400°C~500°C of the traditional titanium alloy to about 650°C~700°C [21, 22]. Typically, the Ti2AlNb alloys are composed of 20 to 30 Al and 12.5-30 Nb. The proportion of Nb has decided the microstructure and mechanical properties due to the different phases during heat treatment process. The yield stress and ultimate tensile stress of the Ti2AlNb-based alloys might approach 845 MPa and 1002 MPa, respectively, at 650°C [21]. However, one particular concern is that it is more sensitive to notches. In this scenario, the Ti2AlNb alloys are implemented in the blisk structure. At first, the forging blank including the blade/disc was manufactured according to the designed component size. Afterwards, the blisk was obtained after a series of

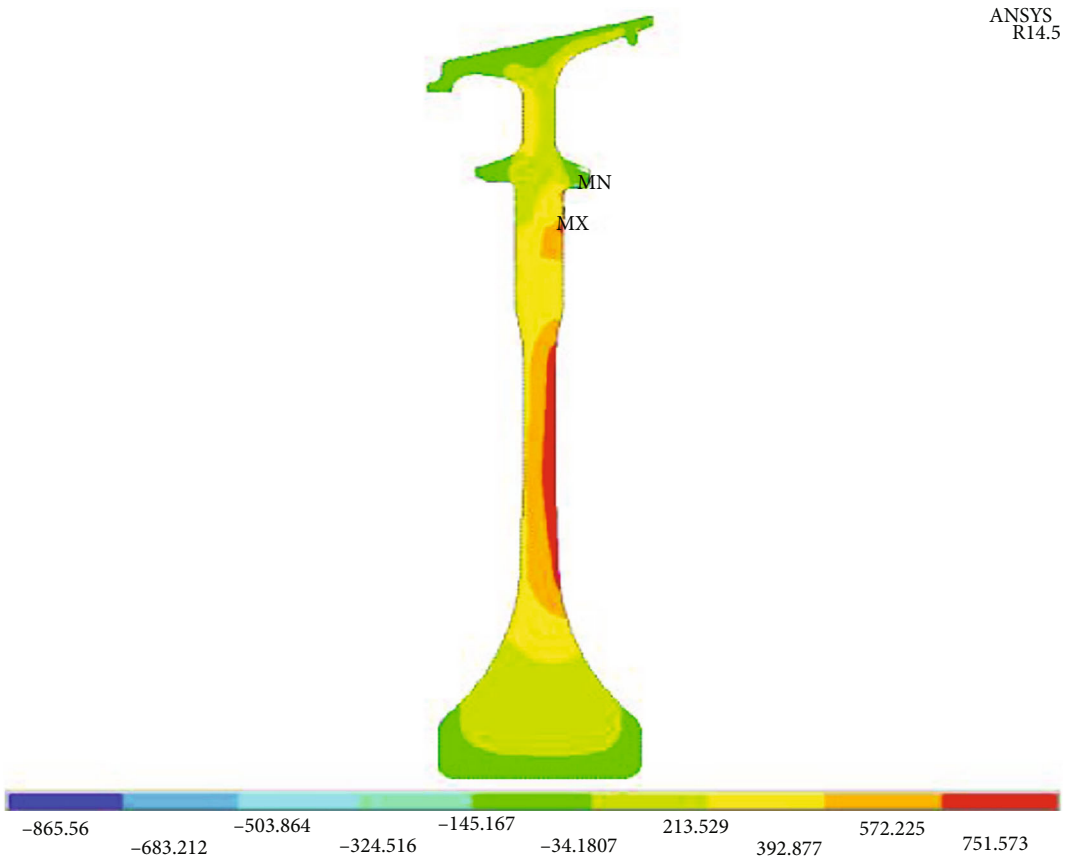

Figure 8: Radial stress distribution.

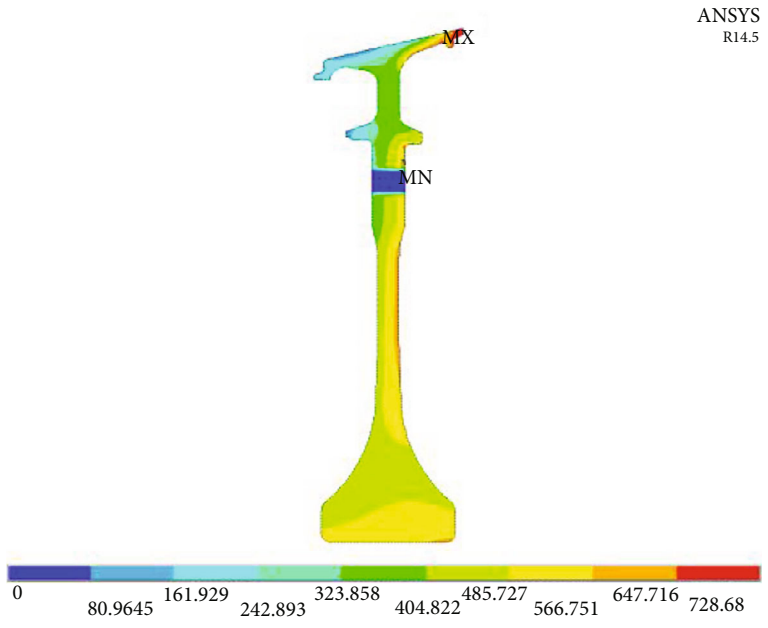

Figure 9: Circumferential stress distribution.

manufacturing process, including rough turning, finish turning, polishing, clamp repair, and flame plating. In order to explore the possibility of applying Ti2AlNb material in aero-engines and validate the burst speed limit for certification purposes, three approaches were incorporated to estimate the burst speed of the optimized blisk.

3.1. Mean Stress Method. One commonly accepted approach is the mean stress (MS) method considering the burst speed factor [23, 24]. It is a semiempirical method dependent on the engineers' experience. The main principle is to perform the finite element analysis, then utilize the mean stress and correction coefficient to calculate the burst speed. The burst speed factor is listed in the following equation:

$$k_b = \sqrt{\frac{k\sigma_b}{\sigma}}, \tag{4}$$

where k_b is the burst speed safety factor, σ_b is the ultimate tensile strength, σ represents the mean stress for maximum allowable speed, and k is the correction coefficient.

This approach provides convenient access for burst speed calculation once the finite analysis results are known. However, the prediction of circumferential burst speed is quite different from the radial burst speed with regard to the selection of correction coefficient. When calculating the circumferential burst speed, the mean circumferential stress calculation should consider the uneven stress distribution resulting from the geometry and material dispersion, which lead to the area-weighted approach according to the meridian plane. Typically, the correction coefficient k is lower than 1. Nevertheless, the radial burst speed is estimated under the assumption that the radial stress is uniformly distributed as well as the material properties. Hence, k is usually chosen as 1. It should be noted that for a compressor disc, the thinner thickness makes the CRS more accurate in the radial burst speed prediction using the mean stress method.

The disc stress was calculated using the two-dimensional axisymmetric finite element model with the design point stress distribution depicted in Figures 8 and 9. It could be seen that the maximum radial stress and circumferential stress are larger than 700 MPa. Nevertheless, the mean stress of the meridian plane was obtained by dividing the total force by the total area of the meridian plane. The total force of the meridian plane was achieved using the weighted integral approach. It should be noted that the bolt holes using the plane stress element with thickness need to be excluded from the model during the circumferential stress calculation. However, considering the nonuniformity of stress distribution in the meridian plane, the range of the coefficient k for the meridian plane burst speed analysis was confirmed to be between 0.86 and 0.93. As discussed previously, k is set as 1 for the cylindrical plane burst speed calculation. In this scenario, the burst speed safety factor should be larger than 1. Therefore, the burst speed could be estimated with the results listed in Table 5. Obviously, the weak point is the cylindrical plane resulting from the high radial mean stress. The estimated burst speed is 21179 r/min with the rupture originated from the web radial stress.

Regarding the uneven distribution of the meridian plane circumferential stress and cylindrical plane radial stress, the mean stress has to be corrected to cater to the nonuniform stress. Besides, material discretion also needs to be considered. Nevertheless, the selection of the correction coefficient highly depends on the designer and the database for engineering practice has not been established. Consequently, it might lead to the apparent deviation of the predicted burst speed and the experimental speed. Furthermore, the prediction of the burst speed using MS for the bolt holes, transition fillet, and groove bottom regions is limited due to the high non-axis-symmetrical stress concentration.

Table 5: Burst speed results from mean stress method.

Weak position	k	Mean stress (MPa)	Burst speed (r/min)
Meridian plane	0.93	462	22498
	0.86	462	21635
Cylindrical plane	1.0	561	21179

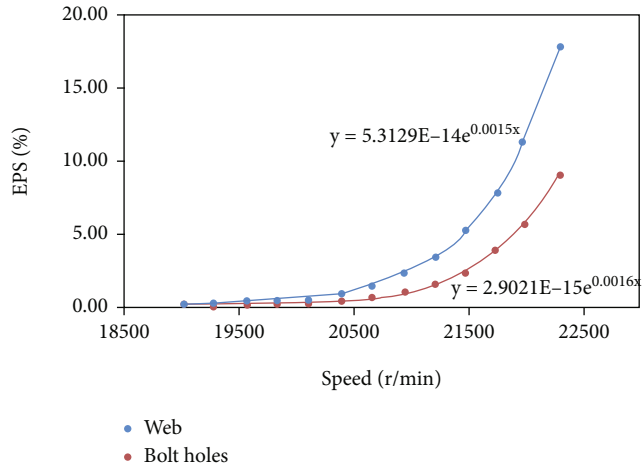

Figure 10: Fitted curves for EPS versus rotational speed.

Table 6: Burst speed results from local stress and strain method.

Weak point	EPS (%)	Burst speed (r/min)
Web	8.984	21841
Bolt hole	8.984	22293

3.2. Local Stress-Strain Method. The material elongation could describe the ability of the material to withstand plastic deformation before encountering failure. According to the local stress-strain (LSS) method [25, 26], the fracture criterion of the disc can be further expanded. When the equivalent plastic strain (EPS) of any local point in the disc reaches the allowable elongation of the material under the monotonously increasing rotational speed, then the rotational speed is identified as the disc rupture speed. The EPS is expressed in the form of logarithm and should be lower than the elongation, as shown in the following equation:

$$\varepsilon_{\ln} \le \ln(1 + \delta_5). \tag{5}$$

It means that when the EPS of any location in the disc exceeds the material elongation, then the crack is generated and propagates quickly, leading to the burst of the disc. The elastic-plastic stress-strain cure was obtained according

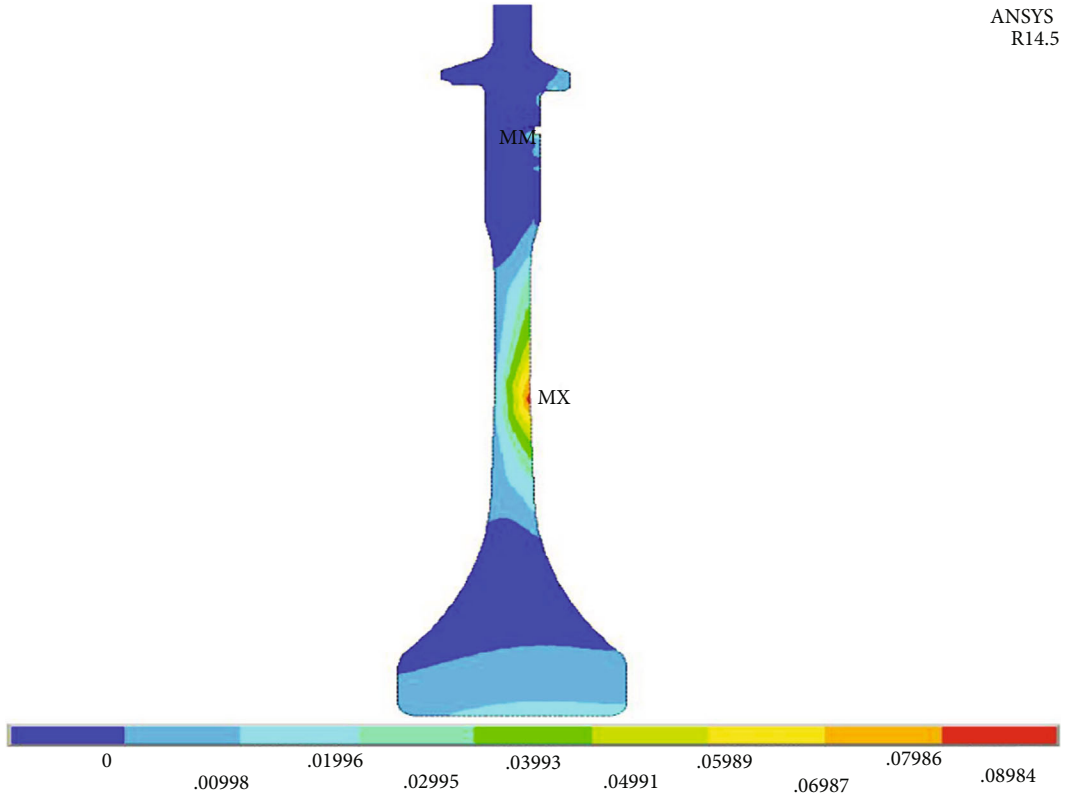

Figure 11: Web EPS distribution.

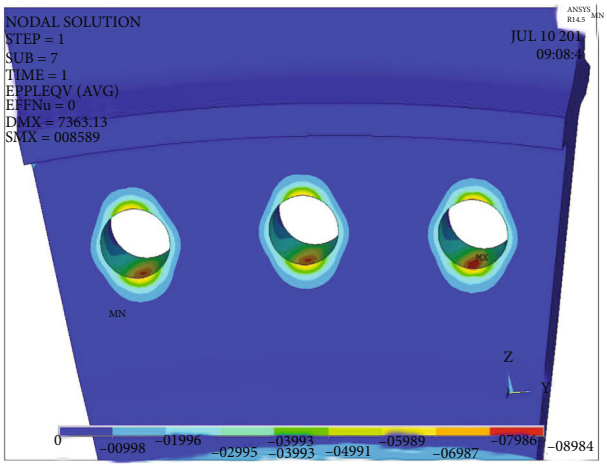

Figure 12: Bolt hole EPS distribution.

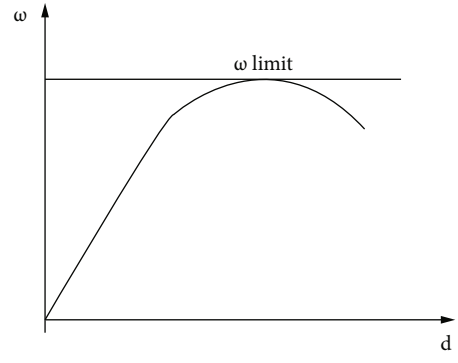

Figure 13: Rotational speed variation versus radial deformation.

to the uniaxial tensile specimen results. Then, the elastoplastic curve of the material is fitted by von Mises yield criterion using the finite element software.

In this scenario, the EPS-speed curve was fitted by increasing the rotational speed and calculating the corresponding EPS. The most concerning parts of the disc are the web and the bolt holes. The maximum allowable EPS is 8.984% before the disc encounters failures. The experimental points and the corresponding fitted EPS-speed curve are depicted in Figure 10. It could be seen that the web EPS shows significant growth from 3.44% to 17.89% when the rotation speed goes up from 21200 r/min to 22300 r/min. However, the maximum bolt hole EPS for 22300 r/min is 9.06%, which lies around the logarithmic elongation limit. By using the equation depicted in Figure 10, the predicted burst speed for the web and bolt hole is demonstrated in Table 6. Apparently, the web is more dangerous than the bolt hole with an estimated burst speed of approximately 21841 r/min. Figures 11 and 12 show that the weak point of the web and bolt hole with the maximum EPS reaches maximum allowable elongation.

3.3. Global Plastic Instability Method. The global plastic instability (GPI) method [15, 27, 28] assumes that the rupture process of aeroengines under the centrifugal load is

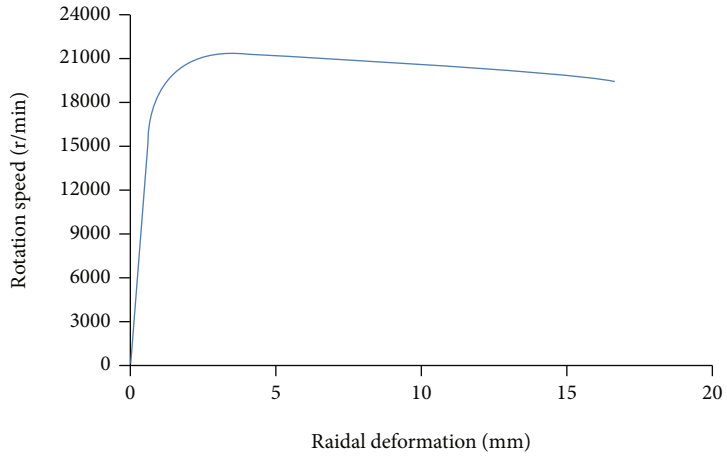

Figure 14: Rotational speed versus radial deformation.

similar to that of smooth specimens and notched specimens. The disc would encounter the global plastic instability when it reaches a certain rotational speed, which leads to the burst of the blisk due to the plastic deformation.

In the disc overspeed experiment, the radial deformation is growing when rotational speed gradually increased. Under the assumption that the deformation in the radial direction is uniform, the variation of rotational speed versus the disc radial dimension could be observed, which is similar to the tensile response curve obtained by controlling displacement loading of smooth and notched specimens. There exists a maximum allowable speed that the disc would not bear any more load after exceeding the speed due to the plastic instability. The rotational speed has to be lowered to maintain the balance, as shown in Figure 13.

Considering the complex disc shape and heavy loading, a large deformation would be expected when reaching the burst speed. Therefore, the finite element analysis considering the large nonlinear deformation was adopted in the burst speed prediction process. The simulated result of the radial deformation versus rotational speed is depicted in Figure 14. It shows the same trend as Figure 13 with the maximum allowable rotation speed of 21440 r/min and the corresponding radial deformation about 4.5 mm.

4. Validation and Discussion

On completion of the burst speed calculation, the disc burst experiment was conducted in Zhejiang University High-Speed Rotating Machinery Laboratory to validate the numerical results. The experimental temperature is room temperature with the test performed in a vertical rotational rig. In addition, the test was recorded and monitored by a high-speed camera. Figure 15 depicts the detailed rupture process of the investigated blisk. What can be seen clearly is that there existed a radial crack in the first picture, and then, it propagated and expanded rapidly. In the second picture, a circumferential crack was found near the radial crack, which seemed to be the maximum web EPS point in Figure 11. After that, the crack propagated quickly until the disc burst into pieces, as shown in the third and fourth picture.

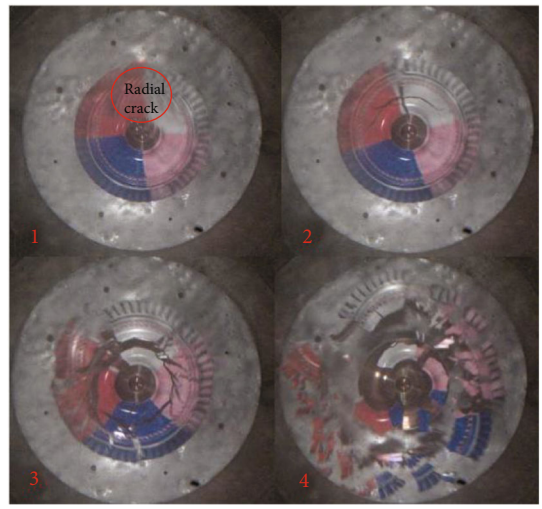

Figure 15: Rupture process of the investigated blisk.

As revealed earlier, the Ti2AlNb material is quite sensitive to notches or cracks. Once the web EPS reaches the upper bound, the blisk encounters rupture in seconds. Meanwhile, the final rupture state indicates that the material is relatively weak in brittleness and toughness at room temperature. It should be carefully designed in the application of high-speed turbomachinery.

Figure 16 compares the burst speed between the numerical calculation and experimental results. The tested burst speed was 20935 r/min, as the black bar indicates. Meanwhile, the estimated burst speed from MS method, LSS method, and GPI method was 1.17%, 4.33%, and 2.41% higher than the experimental value. The errors are believed to be acceptable if less than 5%. It should be noted that the reason why the MS method is accurate than other methods is that the correction coefficient was defined as 1, which suits the thin disc web condition. The real correction coefficient inferred from the test results is about 0.98, which is very close to the defined value. However, it should be pointed out that the MS method is highly dependent on experience or data from similar structures and materials. Finally, the

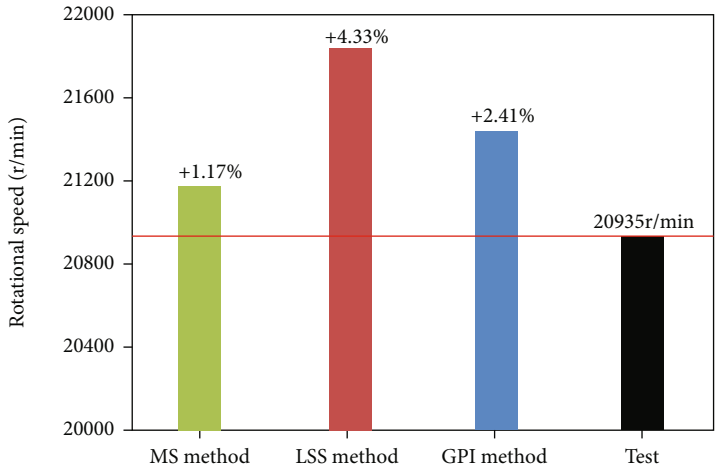

Figure 16: Burst speed comparison.

rupture mode predicted by the three methods was web failure in the radial direction, which is consistent with the experimental results.

5. Conclusions

A comprehensive investigation on the design optimization and burst speed prediction of a Ti2AlNb blisk has been performed. The adopted DOE approach provides a convenient way to reduce the design iterations using the OLHD method to generate the sampling points. Meanwhile, the geometric model is updated and evaluated simultaneously in the Workbench software, which simplified the optimization process. The achieved lowest disc weight is 15.2 kg with the BCS safety factor reaching the minimum allowable value. In addition, it should be pointed out that the bore width, bore angle, and web width are identified to be the most influential factors that affect the safety factors and the disc weight. Increasing the bore width and web width could significantly improve the safety factors but burden the disc weight whereas the rise of bore angle shows the opposite trend.

After obtaining the optimized blisk, three methods have been included to predict the burst speed. It has been found that the mean stress method offers the most precise results only when the correction coefficient is given properly, which relies on engineers' experience. The LSS method and GPI method also predict the burst speed accurately with errors less than 5%. It could be observed in the experimental results that the disc encountered failure starting from the radial direction in the web, which was forecast in the numerical calculation.

Further studies need to be undertaken considering the thermal load with regard to the HPC last stage compressor. Design optimization using the 3D analysis for the blisk would be further investigated in the future.

Abbreviations

d: Radial deformation (unit: mm)
DOE: Design of experiment
h: Bore height (unit: mm)
k: Correction coefficient
n: Safety factor
N: Contribution rate (unit: %)
w: Bore width (unit: mm)
w_1: Web width (unit: mm)
w_2: Neck width (unit: mm)
θ: Bore angle (unit:°)
θ_1: Web angle (unit: °)
BCS: Bore circumferential stress (unit: MPa)
CRS: Cylindrical radial stress (unit: MPa)
CSCS: Cylindrical surface circumferential stress (unit: MPa)
EPS: Equivalent plastic strain
GPI: Global plastic instability
MPCS: Meridian plane circumferential stress (unit: MPa)
MS: Mean stress
LSS: Local stress-strain
OLHD: Optimal Latin hypercube design.

Greek Symbols

σ: Tensile stress (unit: MPa)
β: Coefficient
ε: Equivalent plastic strain in logarithm (unit: %)
ω: Rotational speed (unit: (r/min)).

Subscripts

0.2: 0.2% proof strength
b: Ultimate strength
r: Radial
θ: Circumferential.

Data Availability

The raw/processed data required to reproduce these findings cannot be shared at this time as the data also forms part of an ongoing study.

Conflicts of Interest

The authors declare that they have no conflicts of interest.

Acknowledgments

The authors would like to thank AECC Shenyang Engine Research Institute for the fund and support. The authors would like to thank Zhejiang University High-speed Rotating Machinery Laboratory for their help.

References

[1] C. Guang, "The application of blisk structure on foreign engines," *Aeroengine*, vol. 1, pp. 1–6, 1999.

[2] L. Kasina, R. Kotur, and G. Gnanasundaram, "Minimum weight design of aero engine turbine disks," in *Proceedings of the ASME 2015 Gas Turbine India Conference. ASME 2015 Gas Turbine India Conference*, Hyderabad, India, 2015.

[3] Q. Xiaodong and S. Xiuli, "Multidisciplinary design optimization of turbine disks based on ANSYS workbench platforms," *Procedia Engineering*, vol. 99, pp. 1275–1283, 2015.

[4] A. R. Rao, J. P. Scanlan, and A. J. Keane, "Apply multi-objective cost and weight optimization to the initial design of turbine disks," *Journal of Mechanical Design*, vol. 129, no. 12, pp. 1303–1310, 2007.

[5] L. W. Li and S. Lu, "Structure optimum design techniques for multi-web fan disk based on ANSYS," *Journal of Aerospace Power*, vol. 26, no. 10, pp. 2245–2250, 2011.

[6] S. Lu and F. J. Lu, "Structure optimization design for blisk based on ANSYS," *Journal of Aerospace Power*, vol. 27, no. 6, pp. 1218–1224, 2012.

[7] Y. X. Liu, P. H. Cong, Y. W. Wu, J. L. Li, and X. P. Wang, "Failure analysis and design optimization of shrouded fan blade," *Engineering Failure Analysis*, vol. 122, article 105208, 2021.

[8] Z. J. Huang, C. G. Wang, J. Chen, and H. Tian, "Optimal design of aeroengine turbine disc based on kriging surrogate models," *Computers & Structures*, vol. 89, no. 1-2, pp. 27–37, 2011.

[9] A. Bharatish, P. V. Srihari, A. Panchal, and H. N. Narasimhamurthy, "Analysis of fir tree root of aero-engine disc assembly for simultaneous optimization of fretting characteristics," *Journal of The Institution of Engineers (India): Series C*, vol. 100, pp. 859–868, 2019.

[10] D. Mavroudi, A. Kalfas, A. Abenhaim, and H. Moustapha, "Design optimization of aero-engine turbine blade and disc fixing," *Aeronautics and Aerospace Open Access Journal*, vol. 3, no. 2, pp. 106–113, 2019.

[11] C. H. E. N. Guang, *Structural Desing and Analysis of Aeroengine*, Beijing University of Aeronautics and Astronautics Press, Beijing, 2006.

[12] B. Manavi, "Centrifugal rotor tri-hub burst for containment system validation," in *Proceedings of the ASME Turbo Expo 2006: Power for Land, Sea, and Air. Volume 5: Marine; Microturbines and Small Turbomachinery; Oil and Gas Applications; Structures and Dynamics, Parts A and B*, pp. 661–669, Barcelona, Spain, May 2006.

[13] M. Mazière, J. Besson, S. Forest, B. Tanguy, H. Chalons, and F. Vogel, "Overspeed burst of elastoviscoplastic rotating disks: part II - burst of a superalloy turbine disk," *European Journal of Mechanics - A/Solids*, vol. 28, no. 3, pp. 428–432, 2009.

[14] A. N. Servetnik, "Energy-based method for gas turbine engine disk burst speed calculation," in *28th Congress of the International Council of the Aeronautical Sciences (ICAS2012)*, vol. 3, pp. 2443–2448, Brisbane, 2012.

[15] H. Ekhteraei Toussi and F. M. Rezaei, "Elasto-plastic deformation analysis of rotating disc beyond its limit speed," *International Journal of Pressure Vessels and Piping*, vol. 89, pp. 170–177, 2012.

[16] B. H. Maruthi, M. V. Reddy, and K. Channakeshavalu, "Finite element formulation for prediction of over-speed and burst-margin limits in aero-engine disc," *International Journal of Soft Computing and Engineering*, vol. 2, no. 3, pp. 172–176, 2012.

[17] N. Squarcella, C. M. Firrone, M. Allara, and M. Gola, "The importance of the material properties on the burst speed of turbine disks for aeronautical applications," *International Journal of Mechanical Sciences*, vol. 84, pp. 73–83, 2014.

[18] R. G. Alderson, M. A. Tani, and R. J. Hill, "A three-dimensional approach to the optimization of a gas turbine disc and blade attachment," in *11th Propulsion Conference*, Anaheim, CA, USA, 1975.

[19] J. D. Mattingly, W. H. Heiser, and D. T. Pratt, *Aircraft engine design 2nd edition*, AIAA Education Series, Washington, 2002.

[20] R. R. Cairo and K. A. Sargent, "Twin web disk:a step beyond convention," *Journal of Engineering for Gas Turbines and Power*, vol. 124, no. 2, pp. 298–302, 2002.

[21] W. Chen, J. W. Li, L. Xu, and B. Lu, "Development of Ti2AlNb alloys: opportunities and challenges," *Advanced Materials and Processes*, vol. 172, no. 4, pp. 23–27, 2014.

[22] P. Zhang, Q. Zhu, and H. Qin, "Research progress of high temperature materials for aero-engines," *Material Report*, vol. 28, no. 6, pp. 27–31, 2014.

[23] Aeroengine Design Manumal Editorial Board, *Aeroengine design manumal: Volume 18*, Aviation Industry Press, Beijing, 2001.

[24] S. Murthy and Shivarudraiah, "Verification of over-speed and burst margin limits inaero engine rotor coupling along with estimation of low fatigue life," *International Journal of Applied Engineering Research*, vol. 13, no. 20, pp. 14498–14504, 2018.

[25] J. Y. Wan and B. Z. Zho, "Elastic-plastic disk burst criteria establishment and variabale thickness disk burst rotational speed prediction," *Aeroengine*, vol. 37, no. 5, pp. 4–7, 2011.

[26] H. H. Li, K. M. Wang, C. C. Zhang, W. G. Wang, and G. G. Chen, "Prediction of rotor burst using strain-based fracture criteria to comply with the engine airworthiness regulation," *Journal of Engineering for Gas Turbines and Power*, vol. 143, no. 7, article 071003, 2021.

[27] A. N. Eraslan and H. Argeso, "Limit angular velocities of variable thickness rotating disks," *International Journal of Solids and Structures*, vol. 39, no. 12, pp. 3109–3130, 2002.

[28] M. Maziere, *Over speed burst of turbo engine disks, [Ph.D. thesis]*, Mines Paris–Paris Tech, Paris, 2006.